Published December 1, 1987

Protein Sorting among Two Distinct Export Pathways Occurs from the Content of Maturing Exocrine Storage Granules

Mark von Zastrow and J. David Castle

Department of Cell Biology, Yale University School of Medicine, New Haven, Connecticut 06510

Abstract. We have developed a method for separating purified parotid secretory granules according to their degree of maturation, and we have used this method to examine the relationship between granule formation and stimulus-independent (constitutive) protein secretion. Constitutive export of pulse-labeled secretory proteins occurs almost entirely after their appearance in newly formed granules, and this secretion can be resolved kinetically into two distinct components. Later-phase secretion is the more prominent component and, according to kinetic and compositional criteria, appears to result from basal exocytosis of mature granules. In contrast, early-phase secretion (1.5–15% of constitutive protein output) appears to originate from maturing granules but differs significantly from granule content in composition; that is, the early component exports individual protein species in different relative amounts. Maturing granules, which are labeled most highly before and during the appearance of early-phase secretion, possess numerous coated membrane evaginations suggestive of vesicular traffic. We propose that, in addition to basal exocytosis of relatively mature granules, constitutive exocrine secretion results from limited, selective removal of content proteins from forming and maturing granules. Thus protein sorting and packaging occur together in granule compartments. Exocrine secretory granules constitute an extension of the post-Golgi sorting system and are not merely terminal depots for proximally targeted polypeptides.

EUKARYOTIC cells can secrete proteins in a regulated (acutely stimulus-dependent) or constitutive (stimulus-independent) manner, and it is clear that regulated secretion occurs by stimulus-amplified exocytosis of stored secretory granules (33). During the past several years it has been emphasized that cells that express regulated secretion also discharge proteins in a constitutive manner (21). Depending on the cell type examined, this stimulus-independent export is thought to involve two types of pathways. In transformed endocrine cells a rapid Golgi-based vesicular route that is independent of granule exocytosis and exports a different spectrum of polypeptides than is stored in granules has been implicated (reviewed in 21). Nontransformed endocrine cells also release major granule content components in a relatively rapid and stimulus-independent manner but, in these cells, such export is thought to result from preferential exocytosis of younger secretory granules (e.g., 14). In nontransformed exocrine cells there may be more than one constitutive export route, one which most probably involves granule exocytosis and at least one other whose intracellular origin has not been elucidated (1, 6).

In view of the general suggestion from morphologic studies that granule maturation is associated with vesicular traffic (10, 16), we have been interested for some time in a possible relationship between granule maturation and nongranular protein secretion. We have addressed this question in parotid acinar cells, a regulated exocrine cell type whose secretory behavior can be studied readily in tissue preparations and whose subcellular components can be isolated in purified fractions. Of central importance to this study, we have developed a procedure for separating secretory granule subpopulations according to their degree of maturation. Precursor–product relationships between less and more dense subpopulations have been shown by fractionation of tissue that was labeled biosynthetically in a pulse–chase protocol. Parallel analysis of unstimulated secretion of radiolabeled polypeptides has identified two kinetically distinct phases of discharge. We show that the early phase begins after the appearance of newly synthesized secretory proteins in the content of relatively immature granules occurs concurrently with granule maturation, and is kinetically incompatible with origin from pregranular (i.e., Golgi) compartments. Compositionally, early-phase secretion is found to export the full spectrum of granule content proteins, but in relative amounts that differ substantially from those present in maturing granule compartments. Thus it appears to originate from the content of maturing granules but its composition cannot be explained by exocytosis of these granules. In contrast, later-phase secretion, which accounts for the majority of constitutive export of all proteins examined, is shown to be kinetically and compositionally consistent with an origin from basal exocytosis of relatively mature granules. Thus the two phases reflect distinct constitutive export pathways

Dr. von Zastrow's present address is the Department of Psychiatry, Stanford University Medical School, Palo Alto, CA 94304. Dr. Castle's present address (to which reprint requests should be sent) is the Department of Anatomy and Cell Biology, University of Virginia Medical Center, Box 439 Jordan Hall, Charlottesville, VA 22908.

Published December 1, 1987

evolving from maturing secretory granules. Because numerous coated evaginations mark forming storage granules, we suggest that the early phase comprises a vesicle-mediated route to the cell surface. Because the cargo is selective among the major granule content proteins, we conclude that the forming exocrine granule participates in post-Golgi sorting operations.

Materials and Methods

Resolution of Secretory Granule Subpopulations by Isosmotic Density Gradient Centrifugation

Rationale. Granule maturation involves progressive concentration of intragranular proteins well beyond levels attained in proximal Golgi and condensing vacuole compartments (19, 28). This concentration process is expected to cause an increased buoyant density of the granule (ρ_{gr}) according to the following equation rewritten from reference 37: $\rho_{gr} = 1 + C(1 - v_{pr})$, where v_{pr} is the partial specific volume of content protein (~0.75) and C is internal protein concentration. (Membrane contributions, <1% of granule mass and volume, are neglected.) Because parotid granules behave as osmometers, readily losing internal water and contracting to a lower-limit volume (and, therefore, upper-limit density) in hyperosmotic media (4), we sought to minimize such osmotic perturbation of ρ_{gr} by using isosmotic fractionation conditions. Self-formed Percoll gradients in isosmotic sucrose solutions provide shallow, continuous density gradients of low viscosity, capable of resolving small density differences with relatively rapid approach to isopycnic equilibrium (27).

Method. Parotid glands from male Sprague-Dawley rats (125–150 g) were dissected immediately after animal sacrifice and a 10% wt/vol homogenate and 5% wt/vol postnuclear supernatant were prepared in 0.30 M sucrose, 1 mM sodium morpholino propane sulfonic acid (MOPS), 0.2 mM $MgCl_2$, pH 7.0, as in references 2 and 8. The postnuclear supernatant was supplemented with 1.2 mM EDTA, filtered through 20-μm nylon mesh (Nitex), dispersed by three passes in a loose-fitting Dounce homogenizer, combined with 2 vol of 60% vol/vol Percoll (Pharmacia Fine Chemicals, Piscataway, NJ) in 0.30 M sucrose, 1 mM sodium MOPS, 1 mM EDTA, and centrifuged at 15,000 rpm (16,400 g_{av}) for 30 min in a 70 Ti rotor (spin 1; Beckman Instruments Inc., Fullerton, CA). Granules resolved near the bottom of the centrifuge tube ($\rho > 1.110$ g/ml), whereas most other subcellular components accumulated near the top of the tube and were collected as a mixed fraction ("up" fraction). The granule fraction was collected, adjusted to 60% vol/vol Percoll, and recentrifuged at 25,000 rpm (45,500 g_{av}) for 30 min in a 70 Ti rotor (spin 2). Granules resolved as a continuous distribution and were collected in three fractions ranging in density of Percoll–sucrose medium as follows: fraction 1 (1.115–1.125 g/ml), fraction 2 (1.125–1.140 g/ml), and fraction 3 (>1.140 g/ml). In some experiments fraction 3, which contained the majority of secretory granules, was resolved further by adjusting to 86% vol/vol Percoll in the same isosmotic buffered sucrose solution and recentrifuging at 25,000 rpm for 30 min (spin 3). The resulting continuous distribution was collected as three fractions spanning the density range of 1.140 to 1.158 g/ml (Fig. 1 *a*). By carefully controlling solution concentrations and volumes among experiments, and by collecting fractions according to a standard template, reproducible density cutoffs were obtained. Fractions were diluted with 0.4 M sucrose, 1 mM sodium MOPS, 1 mM EDTA, pH 7.0, and pelleted at low speed (5,000 g_{av} for 60 min) through a layer of buffered 1.0 M sucrose to remove residual Percoll and other soluble contaminants. In certain experiments used to confirm granule content composition, highly purified granules having negligible lysosomal, mitochondrial, or other contaminating membranous elements were obtained by sedimentation through 1.45 M sucrose, 5% wt/vol Ficoll 400 (Pharmacia Fine Chemicals), 2 mM sodium MOPS, 1 mM EDTA, pH 7.0, onto a cushion of 2 M buffered sucrose at 35,000 rpm (150,000 g_{av}) for 90 min in an SW41 rotor (Beckman Instruments, Inc.), (8). Densities of Percoll-sucrose solutions were determined by refractive index, referenced against a series of standards containing known concentrations of Percoll in 0.30 M sucrose, 2 mM sodium MOPS, 1 mM EDTA, pH 7.0, whose densities were measured gravimetrically. The yield of secretory granules collected from the Percoll–sucrose gradients, estimated by recovery of α-amylase activity from the postnuclear supernatant, was ~30%, and the recovery of α-amylase in the sucrose–Ficoll refinement was >90%. Siliconized glassware was used throughout.

Biosynthetic Labeling of Parotid In Vitro

Parotid glands were sliced into ~0.5-mm-thick sections with a Stadie-Riggs knife at 4°C and preincubated at 37°C for 30 min in three changes of methionine-free RPMI medium (Gibco, Grand Island, NY). The slices were then pulse-labeled for 10 min in 10 ml fresh methionine-free medium supplemented with 2 mCi L-[^{35}S]methionine (~800 Ci/mmol, 1 mCi = 37 gBq, New England Nuclear, Boston, MA) washed over 5 min with five complete changes of 15 ml warmed, oxygenated RPMI containing excess (150 mg/liter) L-methionine, and chase incubations (0-min chase was taken to be immediately postpulse) were conducted in 7 ml RPMI containing excess methionine. For secretion experiments, complete medium changes were performed at specified chase times and removed medium was centrifuged at 11,000 *g* for 15 min at 4°C in a microfuge (Beckman Instruments Inc.) to remove traces of cellular debris. For subcellular fractionation experiments, slices were removed at specified chase times, chilled immediately to 4°C, minced with a razor blade, homogenized (Brendler type only), and fractionated as above. All equilibration, washing, and incubation steps were performed in siliconized glassware at 37°C with gentle agitation under a continuous stream of 95% O_2/5% CO_2. Incubation media contained 10 mM sodium Hepes and were adjusted to pH 7.4 under incubation conditions. Secretagogues or antagonists were added as specified in the text. Biosynthetic labeling for autoradiographic localization of radioactivity in subcellular fractions and in parotid acini was performed as described above, except that pulse-labeling was with 2 mCi of a ^{3}H-amino acid mixture (algal hydrolysate; Amersham Corp., Arlington Heights, IL) and 1 mCi [^{3}H]leucine, respectively, and chase media contained the usual amino acid composition of RPMI, in the latter case supplemented with 4 mM leucine.

Electron Microscopy and Autoradiography

Tissue specimens or subcellular fractions were fixed in suspension at 4°C by the addition of one-tenth volume of 30% glutaraldehyde in 0.5 M sodium phosphate, pH 7.4. Postfixation in OsO_4, dehydration, embedding in Spurr medium (EM Science, Cherry Hill, NJ), and preparation of ultrathin sections were performed as in reference 9. Autoradiographic localization of radioactivity in either whole tissue or granule fractions isolated from biosynthetically labeled tissue was performed by overlaying ultrathin sections with photographic emulsion (L4; Ilford, Knutsford, Cheshire, UK), exposing, and developing as described (28). Specimens were examined and photographed with a 301 electron microscope (Philips Electronic Instruments, Inc., Matwah, NJ). Autoradiographic grain distribution over specific structures was determined as described (19).

Biochemical Analyses

One-dimensional electrophoresis of proteins in SDS-PAGE (22) was performed in 1-mm-thick slab gels. Quantitation of resolved components at a chemical level was achieved by densitometric scanning of Coomassie Brilliant Blue–stained gel bands using a scanning densitometer (GS-300, Hoefer Scientific Instruments, San Francisco, CA, or Joyce, Loebl and Co. Ltd., Gateshead, UK) and digital integration of peak areas. Quantitation of radioactivity present in resolved components was performed by excising SDS-PAGE bands, digesting in 20% H_2O_2 at 50°C in sealed tubes, and counting the digest in Optifluor cocktail (Packard Instruments Co., Downer's Grove, IL) using an LS-250 liquid scintillation counter (Beckman Instruments Inc.). Qualitative examination of radioactivity present in SDS gels was accomplished by fluorography as in reference 23.

α-Amylase, UDP-galactosyl transferase, cytochrome *c* oxidase, and *N*-acetyl-β-D-glucosaminidase activities were assayed as summarized previously (8). Protein was determined by reaction with fluorescamine in acetone (35), using BSA as standard.

Results

Separation of Secretory Granule Subpopulations According to Degree of Maturation

A purified fraction of parotid secretory granules (prepared by density gradient centrifugation in spin 1) was separated under isosmotic conditions into a continuous distribution within a density range of 1.115 to 1.158 g/ml, which was divided into standardized density windows (Fig. 1): fractions

Published December 1, 1987

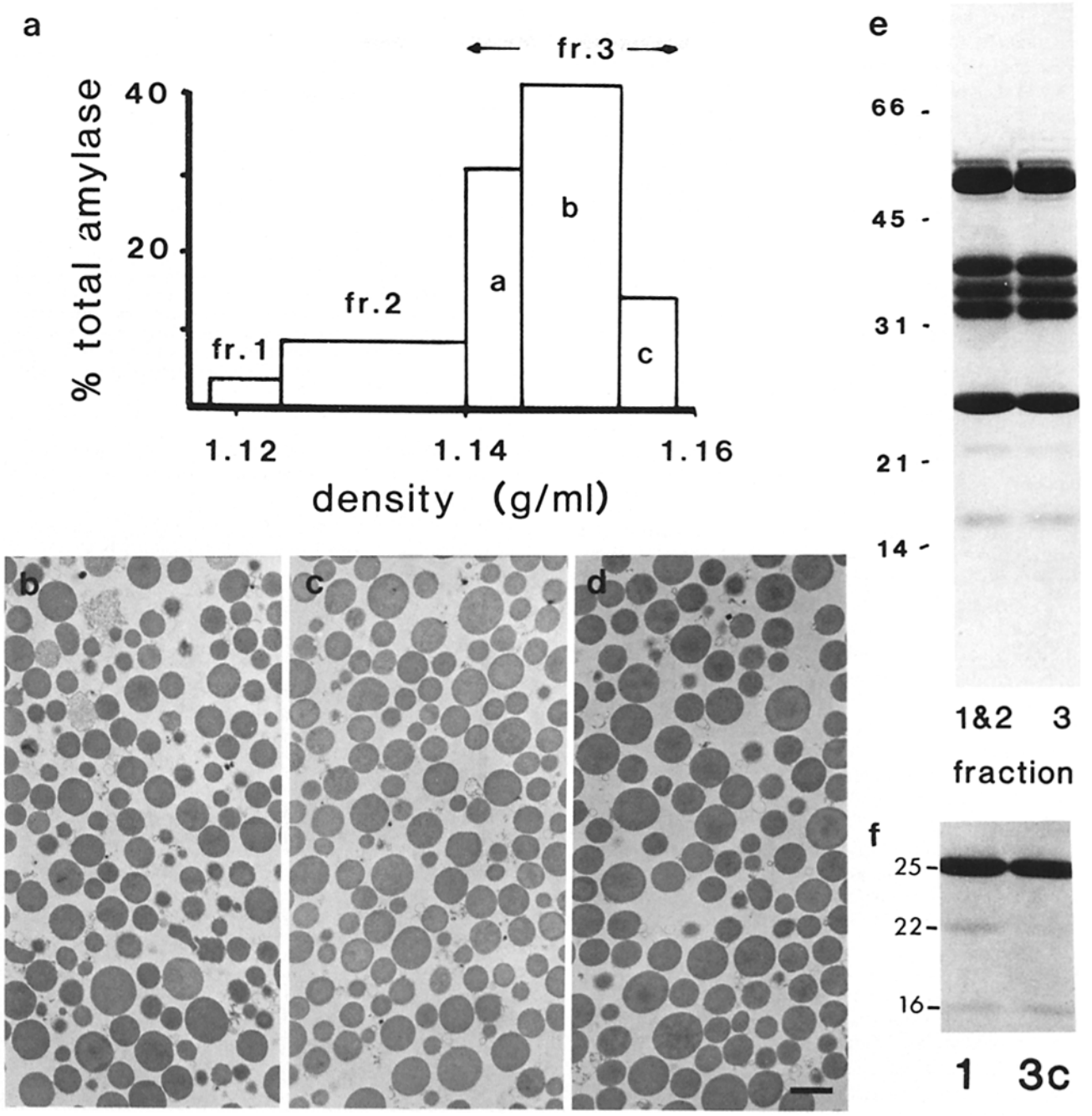

Figure 1. Characteristics of isolated granule subpopulations. (*a*) Density (abscissa) and relative abundance (ordinate; α-amylase enzyme activity) of the subpopulations collected from Percoll–sucrose gradients. For fraction 3 (collected from spin 2), recentrifugation (spin 3) generated fraction 3, *a–c*, resolved over the density range 1.14–1.158 g/cm^3. For fractions 1 + 2 (combined) and fraction 3, intragranular aqueous volume under isosmotic conditions (measured as in reference 4) was 2.49 μl/mg protein and 2.01 μl/mg protein, respectively (SD, <10% of mean). Assuming an intrinsic density of content protein of 1.4 g/cm^3 (12), these measurements correspond to calculated internal protein concentrations of 312 and 367 mg protein/ml total intragranular (aqueous plus protein) volume. By extrapolation to the full density range of granules resolved, the isolated subpopulations differ over a range of ~150 mg/ml in internal protein concentration. (*b–d*) Representative low-power electron micrographs of granule fractions 1–3, respectively, demonstrating the purity achieved by sucrose–Ficoll centrifugation after resolution of subpopulations in isosmotic gradients. Bar, 1 μm. (*e*) Comparative SDS-PAGE (10–15% linear polyacrylamide gradient) of granule fractions 1 + 2 (combined) and fraction 3. Each lane has been loaded with equal enzymatic activity of amylase (the major 58-kD polypeptide), and the resolved proteins are stained with Coomassie Brilliant Blue. The patterns obtained are identical with and without the added sucrose–Ficoll centrifugation used to remove residual minor organelle contaminants (Table I). (*f*) Lower molecular weight region of electrophoretograms (loaded as in *e* and silver stained) of the lowest (fraction 1) and highest (fraction 3c) density subpopulations resolved. This panel identifies a 22-kD band that represents the lone quantitative compositional difference in secretory proteins observed between the granule subpopulations.

Published December 1, 1987

1 and 2 (least dense) and fraction 3 (most dense), with subpopulations 3, *a–c* of increasing density resolvable in a subsequent centrifugation. This distribution resulted from true density heterogeneity within the granule population, because granules collected from various regions of the distribution resolved in spin 2, when recentrifuged under identical conditions, resedimented to their original density (not shown). As well, biophysical measurement revealed that the resolved subpopulations differed as expected in internal protein concentration (see legend, Fig. 1). The purity of the isolated granule subpopulations was assessed biochemically and morphologically. Minimal protein contamination was indicated by the finding that α-amylase, an enzymatic marker of acinar cell secretory granules (32), was found at nearly identical specific activity in all granule fractions and in parotid secretion collected in situ (Table I, legend). More extensive biochemical analysis showed that only the lysosomal marker β-hexosaminidase was detected in the granule fractions at levels of >1% (Table I). This represents an insignificant contamination for studies of content protein composition, because lysosomes occupy <0.5% of acinar cell volume, whereas granules occupy ~30% (17). However, in confirming the identification of granule content components, lysosomal and other membranous contamination could be reduced substantially and efficiently (>90% amylase recovery, Table I) by use of sucrose–Ficoll density gradients developed previously (8) for the isolation of highly purified granule fractions. Morphologically, these fractions were judged to be of high purity, and the corresponding refined and nonrefined fractions exhibited the same protein composition (Fig. 1). All proteins detected in this analysis have been identified previously in granule fractions prepared by other methods and in apical parotid secretion collected in situ (8, 38). Thus the granule fractions are of high purity, adequate for direct biochemical examination of granule components.

To examine whether the granule subpopulations comprise a maturational sequence reflecting progressive concentration of secretory content (20), we pulse-labeled parotid tissue preparations in vitro and examined the kinetics of appearance of labeled secretory proteins in isolated subcellular fractions. These experiments revealed rapid and transient labeling of less dense granule subpopulations, followed by slower accumulation of radioactivity in denser subpopulations (Fig. 2). The least dense granules isolated (fraction 1) labeled most rapidly (maximum accumulation of pulse-labeled protein at 25–55 min chase; Fig. 2 *a*), whereas the densest subpopulation isolated (fraction 3 or, in some experiments, fraction 3 *c*) accumulated labeled secretory proteins most slowly, with continued increase of specific radioactivity even after 3 h chase. EM autoradiographic analysis of isolated granule fractions confirmed that the rapid labeling of less dense granules truly represents radioactivity associated with granule content and cannot be attributed to residual contaminating organelles (Fig. 2 *b*). Notably, this pattern of labeling was observed among the full spectrum of granule content proteins detected (Fig. 2 *c*). However, because of differences detected among individual species in rate of exit from the microsomal fraction and arrival in the granules (probably resulting from heterogenous endoplasmic reticulum (ER)[1] exit rates [29]), we focused further kinetic analysis on α-amylase, a major intragranular protein that could be isolated at high radiochemical purity as an excised band after SDS-PAGE (Fig. 2 *d*). Maximum concentrations of pulse-labeled α-amylase appeared first (<15 min chase) in the spin 1 "up" fraction, a mixed fraction containing ER as well as Golgi elements (Table I), followed successively by transient appearance in less dense granule subpopulations (peak at 0.5–1 h chase) and progressive accumulation in denser subpopulations. This pattern, as well as the crossovers in specific radioactivity observed, is consistent with the compartments represented in these fractions being linked in series in the predominant pathway of secretory protein traffic. Thus less and more dense granule subpopulations, respectively, are enriched in less and more mature granule forms.

Table I. Marker Enzyme Analysis of Subcellular Fractions

Fraction	Recovery from post-nuclear supernate (%)			
	α-Amylase	Galactosyl transferase	Cytochrome oxidase	*N*-Acetyl-β-D-glucosaminidase
Spin 1 "up"	8.0	72	95	34
Fraction 1	1.4 (1.2)	0.6	0.3	7.8 (0.8)
Fraction 2	3.4 (3.2)	<0.01	0.3	6.4 (0.8)
Fraction 3	25.4 (25.0)	<0.01	0.3	5.6 (0.5)

Enzyme activities were measured in subcellular fractions as described in Materials and Methods and are given as percentage of activity present in the parent postnuclear supernatant. Numbers in parentheses refer to recoveries measured in granule fractions that had been refined further by sucrose–Ficoll density gradient centrifugation. Total recovery among all subcellular fractions was 95 ± 8% for all enzyme activities. The specific activities of α-amylase measured in granule fractions 1, 2, and 3 were 2,140, 2,210, and 2,310 U/mg protein, respectively; the specific activity measured in apical secretion collected by cannulation of the parotid duct in situ was 2,250 U/mg.

Least Mature Granule Subpopulations Isolated Represent Early Intermediates in the Process of Granule Formation

To place the granule subpopulations in the time frame of granule formation and maturation observed in situ, we compared the labeling kinetics measured in isolated fractions with those measured by autoradiographic analysis of pulse-labeled tissue specimens. The rate of labeled protein exit from the total microsomal fraction (spin 1 "up") was comparable with the rate measured autoradiographically from ER and Golgi structures (see Fig. 3 *a*); the less complete drainage from the fraction probably resulted from soluble secretory contamination due to granule lysis incurred during tissue homogenization (30). Condensing vacuoles, identified in situ by their low osmium staining density and proximity to the *trans*-Golgi (11, 16), were labeled maximally at 30 min chase. This is comparable with the time of peak labeling of granule fraction 1 (Fig. 2 *a*), although the kinetic resolution of the fractionation analysis does not allow us to say with certainty that nascent condensing vacuoles are represented in the isolated subpopulations. At 60 min chase, when maximum labeling was found in granule fraction 2 (or fractions 1 and 2 combined, Fig. 2, *a*, *c*, *d*), label detected in situ was concentrated over granule structures of higher osmium staining density than condensing vacuoles but which were still located quite close to the Golgi apparatus (Fig. 3 *b*). Frequently, these relatively immature granules possessed coated membrane evaginations (Fig. 3 *c* and inset), suggesting function as a site of vesicular shuttling. At later chase times, more

1. *Abbreviation used in this paper*: ER, endoplasmic reticulum.

Published December 1, 1987

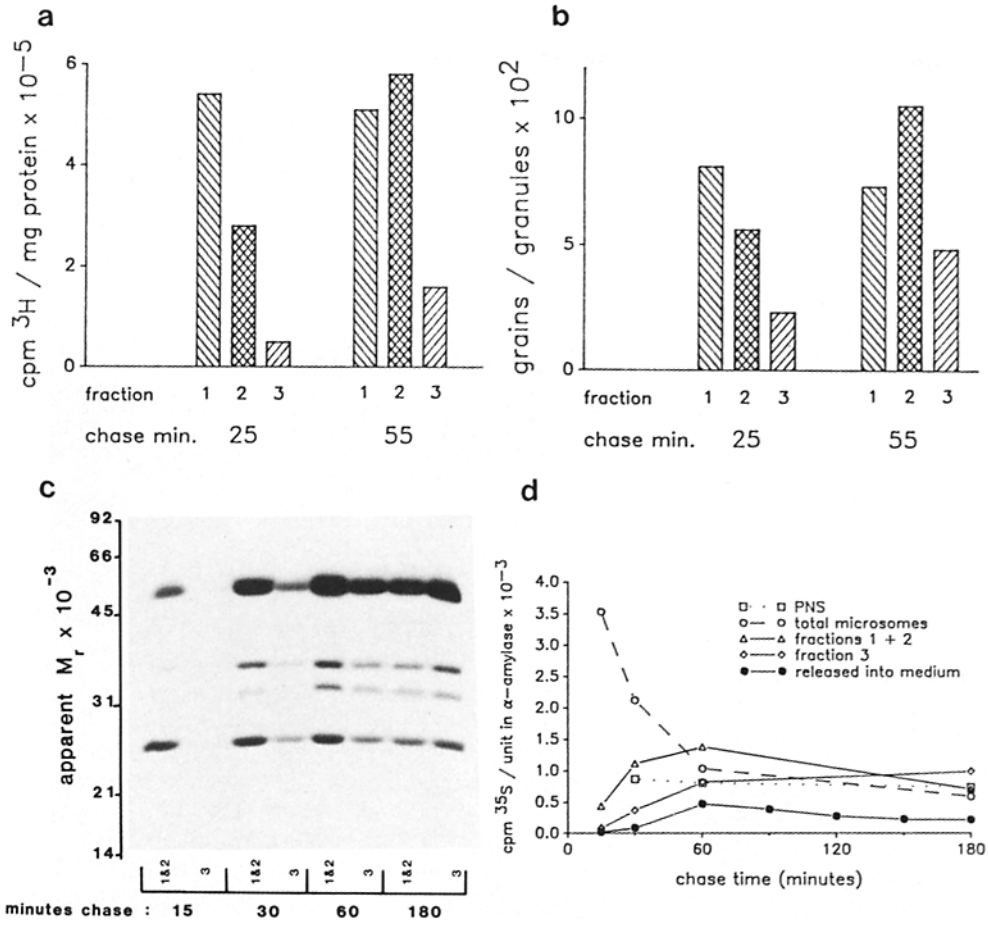

Figure 2. Biosynthetic labeling of granule content proteins and kinetic relationships between cell fractions and unstimulated secretion. (*a* and *b*) Granule subpopulations were investigated at early chase times after pulse-labeling of tissue slices with a ^{3}H-amino acid mixture. The fractions were analyzed in parallel for total protein specific radioactivity (*a*) and by EM autoradiography (*b*). Autoradiographic grains visualized over granule content or within 0.1 μm of the granule perimeter (essentially all grains) were counted and normalized to the total number of granule profiles present in the sections examined. >500 granule profiles were counted per granule fraction. Note the reasonably close agreement between the acid (0.5 N perchloric acid–0.5% phosphotungstic acid) precipitation and autoradiographic measurements, verifying that rapid labeling of lower-density granule fractions truly represents accumulation of newly synthesized proteins in granule content. (*c*) Kinetic behavior of the major parotid secretory polypeptides pulse-labeled with [^{35}S]methionine. Tissue slices were fractionated at the indicated chase times, and granule subpopulations, resolved by isosmotic gradients, were subjected to SDS-PAGE and fluorography; 20 U amylase enzyme activity was loaded per lane. Note that relative to amylase (58 kD), a 25-kD protein (p25) is delivered to less mature granules more rapidly, whereas 32-kD (p32) and 36-kD (p36) polypeptides are delivered more slowly. The precursor–product relationships between fractions 1 + 2 (combined) and fraction 3 can be visualized for each of the bands with increasing chase time. (*d*) Specific radioactivity of amylase in cell fractions and unstimulated secretion (from the same tissue) quantitated from the 58-kD band for samples loaded as in *c*. Rapid drainage from total microsomes (spin 1 "up" fraction) is succeeded by labeling of lower density granule fractions (1 + 2) which in quantitative terms are shown to behave as precursors to higher density fraction 3 granules. Release of pulse-labeled amylase into the incubation medium during chase incubation mostly occurs after accumulation in the immature (fractions 1 + 2) granules and is shown to peak in specific radioactivity at ≥60 min. This phasic behavior occurs in the presence of a constant low rate (<4%/h) of discharge of amylase enzyme activity. Further, comparative kinetic analysis (using linear least-squares fits to semilogarithmic plots of data in this figure to calculate apparent half-times of efflux) distinguishes early-phase secretion as a substantially slower process than microsomal drainage, as discussed in the text. The appearance of early-phase secretion does not differ for parotid tissue slices (used here), lobules, or enzyme-dissociated acini. Thus we are confident that no significant delay (and thus influence on secretory kinetics) is imposed by ductal structures. Finally, note that the specific radioactivity of amylase in early-phase secretion is lower than that of the starting postnuclear supernate or any of the fractions resolved from it.

mature granule structures (of relatively high staining density and located further from the Golgi apparatus) were labeled, and the kinetics of label accumulation in these granules were similar to those measured in more mature granule fractions. Thus the granule fractions represent, with reasonable fidelity, intermediates in the series of granule formation; the least mature subpopulations isolated are kinetically close to nascent condensing vacuoles.

Constitutive Protein Secretion from Parotid Acinar Cells Is Resolved Kinetically into Two Components; the Early Component Originates from Less Mature Granules

Pulse-labeled parotid tissue preparations, incubated in the absence of secretagogues under conditions identical to those used for granule isolation experiments, discharged labeled secretory proteins in two distinct phases. An early secretory phase began at ~30 min post-pulse, peaked over the interval of 1–1.5 h chase, and decreased slowly until ~3.5 h chase, when a second phase of secretion began to appear (Figs. 2 *d* and 4). Addition of secretagogue at 3.5 h (or later chase times) amplified output of labeled secretory protein >30-fold. We did not examine directly the stimulability of early-phase release, because a previous study has shown that isoproterenol preferentially stimulates the discharge of older secretory protein stores and that essentially no stimulated release of biosynthetically labeled proteins occurs until >50 min after pulse (31). The early secretory phase did not result

Published December 1, 1987

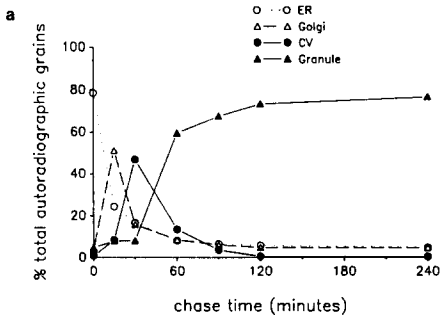

Figure 3. EM autoradiographic analysis of parotid acinar cells pulse-labeled with [^{3}H]leucine. (*a*) Quantitative results obtained at each chase time. Autoradiographic grains present over particular structures are expressed as a percentage of total grains counted at each chase time. (*b*) Representative low power view of an acinar profile at 60 min chase. An acinar lumen (*A*) and several Golgi regions (*G*) are marked. Note the labeling of immature granules located near Golgi structures, which is quite uniform in all cells. (*c*) Higher magnification showing heavy labeling of immature granules near the *trans* aspect of the Golgi at 60 min chase. Note the relative absence of Golgi labeling at this chase time and that heavily labeled immature granules possess coated membrane evaginations (*arrows*). The inset highlights the coat (*arrowhead*) of the granule located at the center of *c*. Bars: (*b*) 2.0 μm; (*c*) 0.5 μm.

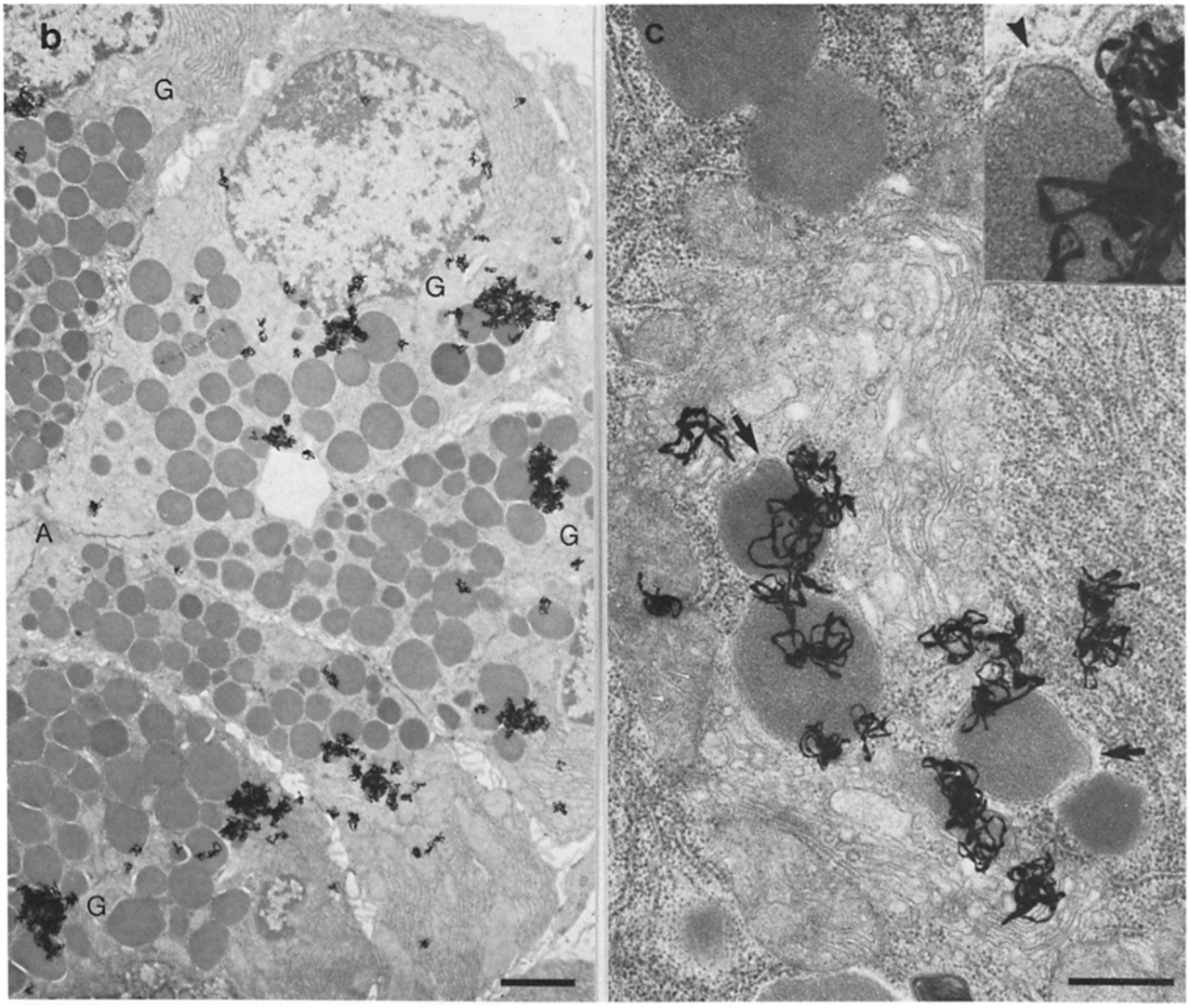

from cell lysis for two reasons: (*a*) the rate of release of cytosolic lactate dehydrogenase remained at a constant, low level (<2%/h) throughout the interval of early-phase release; and (*b*) early-phase secretion contained labeled proteins in relative amounts different from those found in cell lysates (Figs. 4 *a*, 5, and see following text). Both early- and later-phase components were observed even in the presence of adrenergic and cholinergic antagonists (1 μM each phentolamine, propranolol, and atropine), indicating that they did not result from possible residual autonomic stimulation in the preparation. Therefore, both phases represent components of functionally constitutive secretion.

Constitutive secretion exhibits two interesting and important properties in relation to granule formation that can be illustrated most clearly by focusing on the behavior of pulse-labeled α-amylase. First, early-phase secretion is a minor component relative to export of older protein. Approximately 5% of total labeled amylase was discharged in the first 3 h after pulse (Fig. 4 *b*) and, throughout this period, the specific radioactivity of the enzyme recovered from the incubation medium was lower than that measured either in whole cell lysates or in less mature granules (Fig. 2 *d*). Thus the early secretory phase is superimposed on a much larger contribution from constitutive output of older protein. This finding

Published December 1, 1987

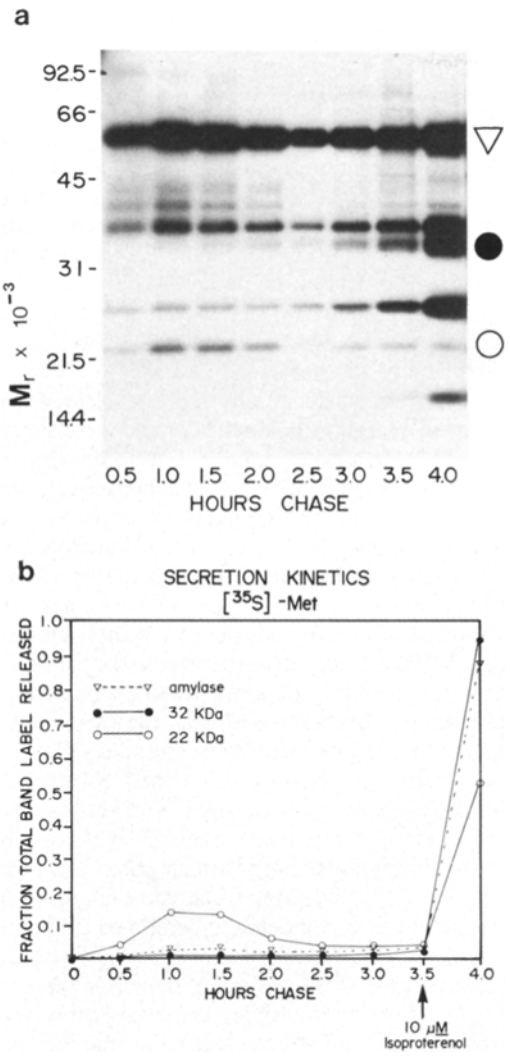

Figure 4. Biphasic protein secretion from parotid acinar cells. (*a*) Fluorograms (SDS-PAGE, 12.5% acrylamide) of [^{35}S]methionine-labeled secretory proteins discharged from parotid slices in successive 30-min chase intervals after a 5-min pulse. Propranolol, phentolamine, and atropine (1 μM each) were present before 3.5 h, at which point 10 μM isoproterenol was added to stimulate granule exocytosis. Gel lanes are loaded according to equal amylase activity (2 U per lane). By visual comparison of specific radioactivities (band intensities) in successive time windows, the early-phase release is evident for each polypeptide; the onset of the second phase is observed in the last interval before β-adrenergic stimulation. (*b*) The corresponding quantitative results for amylase and p32 and p22 polypeptide bands shown in *a*, demonstrating the extremes of relative extent of discharge into the early phase. The isoproterenol-amplified discharge of all species examined signifies that all are components of regulated secretion.

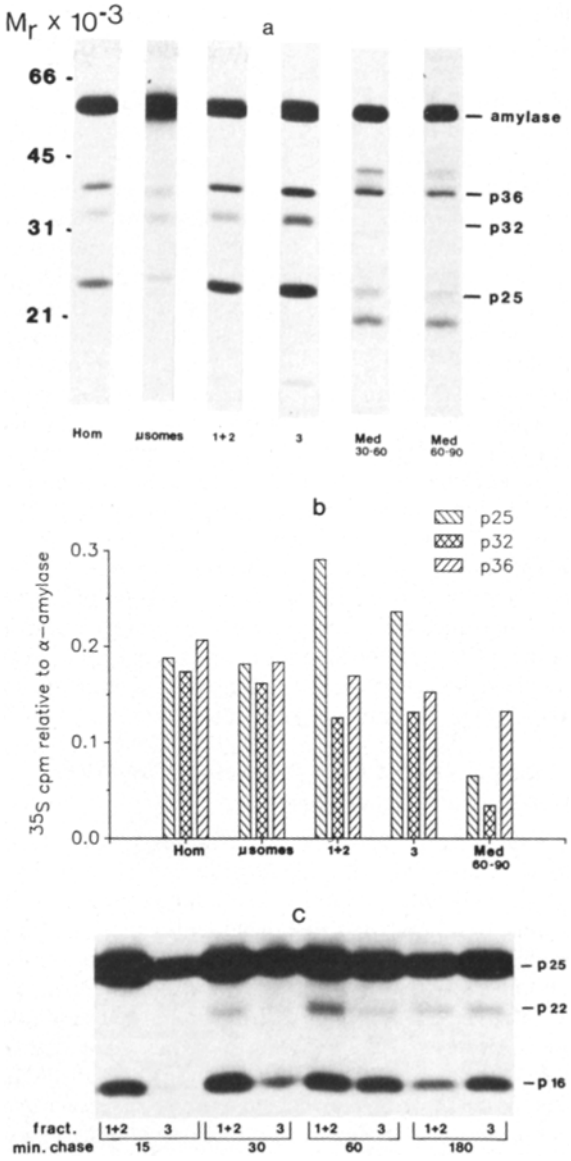

Figure 5. Radiochemical composition of early-phase secretion compared with that of cell lysate, microsomes, and granule content. (*a* and *b*) Medium samples, tissue homogenates, and subcellular fractions from the same [^{35}S]methionine pulse-labeled preparation were resolved by SDS-PAGE (12.5% acrylamide). In *a*, gels were fluorographed, with exposure times adjusted to obtain comparable film density of the amylase band. In *b*, protein bands comprising major secretory species (amylase, p25, p32, p36) were excised and digested; relative incorporation of label is presented as a fraction of that present in amylase isolated from the same samples. All cell fractions were prepared at 60 min chase, and the early-phase secretion samples were collected in the time windows designated. *Hom*, cell lysate (homogenate); *μsomes*, total microsomes (spin 1 "up" fraction); *1 + 2*, less mature granule fractions; *3*, more mature granule fraction; *Med*, secretion at specified chase time interval. (*c*) Fluorographic demonstration that p22 polypeptides, which are most avidly diverted into early-phase secretion, are detected at early chase times (15 min) in granule fractions and mark a precursor–product relationship between less mature (Fraction 1 + 2) and more mature (Fraction 3) granules.

is similar to that observed in exocrine pancreas, where basal exocytosis of relatively mature granules is thought to be the predominant constitutive export route (1, 3). In contrast, this differs from early secretion detected in studies of endocrine cells, where a higher specific radioactivity, thought to represent preferential exocytosis of relatively immature granules, is found (14).

The second property is that labeled protein exported in early-phase secretion most probably originates from the content of forming granules rather than from proximal compartments. By 30 min chase, before a significant amount of labeled amylase had appeared in the medium, a considerable

Published December 1, 1987

amount had exited ER and Golgi compartments and was contained in relatively immature granule forms. This is indicated both by decreased labeled enyzme recovered in the total microsomal fraction and by accumulation in less mature granule subpopulations (Fig. 2 *d*). The general post-Golgi disposition of labeled secretory proteins is also indicated by the in situ autoradiographic analysis (maximum labeling was found in condensing vacuoles at this chase time, before the onset of early-phase secretion, Fig. 3 *a*). Subsequently, peak early-phase output of labeled amylase coincided with (or even followed) its peak appearance in less mature granules. Finally, comparative kinetic analysis at later chase times revealed that the ensuing gradual decrease of early-phase secretion ($t_{½}$, ~80 min) was comparable with the rate of granule maturation measured among the isolated subpopulations but was considerably slower than the rate of drainage of labeled enzyme from the total microsomal fraction ($t_{½}$, ~25 min), which contains ER and Golgi elements (see legend, Fig. 2 *d*). This finding stands in clear contrast to the kinetic similarity that has been observed between protein secretion and exist from ER and Golgi compartments in studies of hepatoma cells, which secrete in a purely constitutive manner (13). Thus the kinetics of onset, peak, and decay of early-phase secretion are most consistent with its origin from the content of maturing granules.

Early-Phase Secretion Does Not Result Directly by Exocytosis of Less Mature Granules

To test whether early-phase secretion resulted directly from exocytosis of newly formed granules, we compared it compositionally with the content of maturational granule subpopulations, which were isolated in the same experiment and at the same chase time. Early-phase secretion contained the full qualitative spectrum of pulse-labeled secretory proteins, but the relative amounts discharged differed substantially from those present in granule content. These quantitative differences, apparent simply by inspection of SDS-PAGE fluorographs (Fig. 5 *a*), were detailed more precisely for major secretory species by liquid scintillation counting of excised gel bands (Fig. 5 *b*). Relative to α-amylase, they were discharged to lesser and differing extents in early-phase secretion. Secreted most sparingly was p32, <1.5% of which was discharged between 0 and 3 h chase (Fig. 4 *b*). This protein (a single ^{35}S-labeled component according to two-dimensional IEF/SDS-PAGE fluorography) comprised ~15% of total of pulse-labeled secretory protein and was detected at essentially identical chemical and radiochemical levels relative to amylase in all granule subpopulations resolved. Other major polypeptides (25 and 36 kD) were secreted in greater amount than p32. In contrast, certain minor species considerably exceeded amylase in relative extent of early-phase secretion. Most notable were 22-kD polypeptides (p22) comprising ~3% of total pulse-labeled protein, of which ~15% was released in the early phase (Fig. 4 *b*).

Although p22 polypeptides are not visualized in the fluorographs of granule fractions shown in Figs. 2 *c* and 5 *a*, which focus attention on the behavior of major secretory proteins, Fig. 5 *c* documents that they are detectable in granule subpopulations as early as 15 min after pulse. Further, they accumulate at longer chase times as bona fide content components in higher-density subpopulations. Consequently, they resemble major secretory polypeptides in being exported primarily (≥85%) in later-phase constitutive secretion or in regulated secretion (≥20-fold amplification in discharge rate in response to β-adrenergic stimulation [Fig. 4]).

The radiochemical composition of early-phase secretion differed not only from that of granules but also from that of all cell fractions examined at all chase times from 15 min to 3 h. It is very unlikely that these findings reflect differential recovery of radiolabeled secreted proteins in the medium (perhaps caused by adsorption or proteolysis artifacts) because early-phase release accompanies discharge of nonradioactive secretory protein that does not vary in composition throughout incubation.

Taken together, these observations indicate clearly that early-phase protein secretion is kinetically most consistent with an origin from maturing granules, but compositional differences involving all secretory proteins apparently preclude exocytosis of less mature granules as its source. Instead, an origin by limited and selective diversion from less mature granule content through vesicle-mediated export seems most likely.

In the latter regard we have considered whether the proteins that are relatively avidly diverted into early-phase secretion become progressively depleted from the content of more mature granules. In the case of p22, the most avidly diverted species, this seems to be the case since Fig. 1 *f* shows that its relative contribution to stained gel profiles decreases dramatically between the least and most dense granule subpopulations. From densitometry of Coomassie-stained electrophoretograms, we estimate that the total amount of p22 is reduced 20–25% (relative to amylase) in granule subpopulation 3 as compared to combined subpopulations 1 and 2. For other granule content proteins we have been unable to detect the small amount of depletion (several percent) predicted. Both by improving the sensitivity of detection of compositional differences and by examining further the most avidly diverted components, we are currently pursuing this apparent maturational depletion in more detail.

Discussion

By focusing on a regulated secretory system that lends itself well to subcellular fractionation, we have studied storage granule formation directly and in parallel with unstimulated protein secretion. Of central importance to this investigation was the development of a density gradient method capable of resolving secretory granules into a continuous distribution of maturational subpopulations, thereby allowing the isolation of a series of purified fractions that are enriched in relatively less or more mature granule forms. The feasibility of such a separation was demonstrated previously, while our studies were in progress, by the finding that a relatively immature subpopulation could be separated by a density step gradient (18). These density differences among subpopulations apparently result from the physiologic increases of internal protein concentration that accompany granule maturation. In the cellular context of granule formation our autoradiographic localization studies have placed the least mature granule forms isolated kinetically close to, but perhaps not fully inclusive of, nascent condensing vacuole compartments. (We suspect that some very immature forms may re-

Published December 1, 1987

solve at even lower density, perhaps not collected in the initial granule fraction isolated in spin 1.)

We have found that unstimulated parotid acinar cells, like pancreatic exocrine cells (1), export pulse-labeled secretory proteins in two readily resolved phasic components. Both components in parotid are observed in the presence of autonomic blockade, and thus represent functionally constitutive secretion. The later one, which contributes the majority of proteins, resembles stimulated secretion in composition and most probably reflects basal exocytosis of storage granules. It is first detectable (although still at relatively low specific radioactivity) after 3.5 h chase (Fig. 4) and peaks at 10–15 h (Scott, M., P. Arvan, and J. D. Castle, unpublished data). In contrast, early-phase secretion is a relatively minor component of constitutive protein output. Peak release of pulse-labeled proteins occurs after 1–1.5 h chase, and this component displays considerable chemical selectivity among individual secretory proteins. All granule content species are represented in early-phase secretion, but they are discharged in relative amounts that differ over a range of ~10-fold. These findings, together with the fact that the kinetics of early-phase protein export are most consistent with its origin from the content of less mature granules, argue that early-phase secretion occurs by limited diversion of secretory proteins from maturing granules. The observation that these granules possess numerous coated evaginations suggests that small vesicles may mediate this alternate export route. Although we have not yet visualized vesicles with appropriate labeling characteristics, it is possible that apical, secretory protein–containing vesicles similar to those described in pancreatic acinar cells (5) might be involved.

Although we are presently not able to rule out the possibility that early-phase discharge of minor secretory proteins might result from preferential basal exocytosis of a compositionally distinct granule population, we are confident for several reasons that such a process cannot explain the differential release of all of the major granule content components. First, these polypeptides are found in very similar amounts in all granule subpopulations isolated, and we have no evidence of even partial resolution of such a putative granule population, which would be expected to differ in amount of all content proteins. Second, our autoradiographic studies of parotid tissue have not detected acinar or ductal cell populations that exhibit granule turnover on the rapid time scale of early-phase secretion. Third, dissociated parotid acini, which are depleted of most ductal structures (not shown), also exhibit early-phase secretion. Finally, previous immunochemical (32), cell fractionation (8, 9), and physiologic (31) studies of the parotid have revealed no evidence of such compositional heterogeneity among or within individual cells.

Recent studies have focused on the reticular *trans*-Golgi network as a probable site of membrane and secretory protein sorting (15, 24), including selective sorting into granule content in regulated secretory cells (21). In the latter regard, the forming granule has been viewed as a terminal recipient of polypeptides. However, morphologic evidence of granule-associated vesicular traffic (included coated membrane evaginations) has been reported in a number of systems (10, 26, 34). These findings have been interpreted primarily in the context of membrane recycling to proximal Golgi elements, although a possible secretory role has been speculated (34). The present results argue strongly that anterograde shuttling of secretory proteins, directed to the cell surface, occurs from forming granules. In addition, the fact that this granule-based diversion appears to be chemically selective leads us to propose that secretory sorting may occur at the level of forming granules, which constitutes a break from the earlier concept that the forming granule serves only as a storage depot.

Because the nascent storage compartment originates in continuity with the *trans*-Golgi reticulum, it is not difficult to envision that sorting operations may extend into forming granules. This may be particularly true in large exocrine granules, where the relatively low surface area/volume ratio may necessitate more prolonged vesicular shuttling to achieve compositional refinement. Mature exocrine granule membrane is highly refined but exhibits some compositional overlap with the apical cell surface (9), so we are currently examining the possibility that anterograde shuttling from forming granules may serve primarily as a vehicle for delivery of membrane components, as may be true in the case of retrograde traffic (17).

The placement of secretory sorting and packaging operations within the same compartment suggests that these processes may be related in mechanism. Because the composition of early-phase secretion differs quantitatively (but not qualitatively) from granule content, we propose that granule-based sorting may entail differing strengths of association of individual protein species with the condensed content, which may be stabilized by noncovalent intermolecular interactions (36, 39). Proteins discharged least in early-phase secretion (such as p32 and p25) would be associated most stably with the condensed content, whereas species diverted in higher amount (amylase, p22's) would be associated less tightly, thereby approaching fluid-phase (or perhaps even membrane-associated) markers of constitutive vesicular traffic. Storage granule formation would then operate by retention in a sorting compartment (possibly analogous to selective retention of polypeptides in the ER [7]), with limited vesicular efflux traffic resulting in the progressive maturational increase of overall protein concentration in the packaged content.

In conclusion, we envision protein sorting in epithelial cells to occur at multiple intracellular sites, in association with the Golgi complex and extending into forming granule compartments. In this regard, it is interesting to note that immature exocrine granules, as well as *trans*-Golgi elements, appear to be relatively acidic compartments (25). Further, we have found recently that the acidotropic agent ammonium chloride disrupts the chemical selectivity of early-phase secretion, without blocking delivery of newly synthesized protein to forming granules (von Zastrow, M., and J. D. Castle, manuscript in preparation). These findings suggest that granule-based sorting, like sorting of soluble proteins at proximal sites, may be a pH-dependent process. In view of the multiple sorting decisions required of regulated epithelial cells (apical vs. basolateral vs. other endomembrane; constitutive vs. regulated), the question of whether granule-based sorting is restricted to a subset of these remains to be explored. If this is the case, granule maturation may provide a particularly favorable model for the examination of a single type of sorting operation.

The authors appreciate the helpful comments of Dr. Richard Cameron and Dr. George Palade on the manuscript and are grateful for the expertise and assistance of Hans Stukenbrok in the EM autoradiographic studies, Ann Curley-Whitehouse in preparation of illustrations, and Lynne Wootton and Chris Flynn in word processing.

This work was supported by a research grant (GM26524) from the National Institutes of Health. Dr. von Zastrow was supported by training grant GM-07205 from the National Institutes of Health.

Received for publication 4 May 1987, and in revised form 27 August 1987.

References

1. Arvan, P., and J. D. Castle. 1987. Phasic release of newly synthesized secretory proteins in the unstimulated rat exocrine pancreas. *J. Cell Biol.* 104:243–252.
2. Arvan, P., and J. D. Castle. 1986. Isolated secretion granules from parotid glands of chronically-stimulated rats possess an alkaline internal pH and inward-directed H+ pump activity. *J. Cell Biol.* 103:1257–1267.
3. Arvan, P., and A. Chang. 1987. Constitutive protein secretion from the exocrine pancreas of fetal rats. *J. Biol. Chem.* 262:3886–3890.
4. Arvan, P., G. Rudnick, and J. D. Castle. 1984. Osmotic properties and internal pH of isolated rat parotid secretory granules. *J. Biol. Chem.* 259: 13567–13572.
5. Beaudoin, A. R., G. Groudin, A. Vachereau, P. St.-Jean, and C. Cabana. 1986. Detection and characterization of microvesicles in the acinar lumen and in juice of unstimulated rat pancreas. *J. Histochem. Cytochem.* 34: 1079–1084.
6. Beaudoin, A. R., A. Vachereau, and P. St.-Jean. 1983. Evidence that amylase is released from two distinct pools of secretory proteins in the pancreas. *Biochim. Biophys. Acta.* 757:302–305.
7. Bole, D. G., L. M. Hendershot, and J. F. Kearney. 1986. Post-translational association of immunoglobulin heavy chain binding protein with nascent heavy chains in nonsecreting and secreting hybridomas. *J. Cell Biol.* 102:1558–1566.
8. Cameron, R. S., and J. D. Castle. 1984. Isolation and compositional analysis of secretion granules and their membrane subfraction from the rat parotid gland. *J. Membr. Biol.* 79:127–144.
9. Cameron, R. S., P. L. Cameron, and J. D. Castle. 1986. A common spectrum of polypeptides occurs in secretion granule membranes of different exocrine glands. *J. Cell Biol.* 103:1299–1313.
10. Castle, J. D., R. S. Cameron, P. Arvan, M. V. Zastrow, and G. Rudnick. 1987. Similarities and differences among neuroendocrine, exocrine, and endocytic vesicles. *Ann. NY Acad. Sci.* 493:448–460.
11. Castle, J. D., J. D. Jamieson, and G. E. Palade. 1972. Radioautographic analysis of the secretory process in the parotid acinar cell of the rabbit. *J. Cell Biol.* 53:290–311.
12. Fasman, G. D. 1976. Handbook of Biochemistry and Molecular Biology: Physical and Chemical Data. Vol. I. 3rd ed. CRC Press, Cleveland. 429.
13. Fries, E., L. Gustafsson, and P. A. Peterson. 1984. Four secretory proteins synthesized by hepatocytes are transported from endoplasmic reticulum to Golgi complex at different rates. *EMBO (Eur. Mol. Biol. Organ.) J.* 3:147–152.
14. Gold, G., M. L. Gishizki, and G. M. Grodski. 1982. Evidence that glucose "marks" cells resulting in preferential release of newly synthesized insulin. *Science (Wash. DC).* 218:56–58.
15. Griffiths, G., and K. Simons. 1986. The trans Golgi network: sorting at the exit site of the Golgi complex. *Science (Wash. DC).* 234:438–443.
16. Hand, A. R. 1971. Morphology and cytochemistry of the Golgi apparatus of the rat salivary gland acinar cells. *Am. J. Anat.* 130:141–157.
17. Hand, A. R., and C. Oliver. 1983. Effects of secretory stimulation on the Golgi apparatus and GERL of rat parotid acinar cells. *J. Histochem. Cytochem.* 32:403–412.
18. Iversen, J. M., D. L. Kauffman, P. J. Keller, and M. Robinovitch. 1985. Isolation and partial characterization of two populations of secretory granules from rat parotid glands. *Cell Tissue Res.* 240:441–447.
19. Jamieson, J. D., and G. E. Palade. 1967. Intracellular transport of secretory proteins in the pancreatic exocrine cell. II. Transport to condensing vacuoles and zymogen granules. *J. Cell Biol.* 34:597–615.
20. Jamieson, J. D., and G. E. Palade. 1977. Production of secretory proteins in animal cells. *Int. Cell Biology Symp., 1976-1977.* B. R. Brinkley and K. R. Porter, editors. 308–318.
21. Kelly, R. B. 1985. Pathways of protein secretion in eukaryotes. *Science (Wash. DC).* 230:25–32.
22. Laemmli, U. K. 1970. Cleavage of structural proteins during the assembly of the head of bacteriophage T4. *Nature (Lond.).* 227:680–685.
23. Laskey, R. A., and A. D. Mills. 1975. Quantitative film detection of 3H and 14C in polyacrylamide gels by fluorography. *Eur. J. Biochem.* 56:335–341.
24. Matlin, K. S. 1986. The sorting of proteins to the plasma membrane in epithelial cells. *J. Cell Biol.* 103:2565–2568.
25. Orci, L., M. Ravazzola, and R. G. W. Anderson. 1987. The condensing vacuole of exocrine cells is more acidic than the mature secretory vesicle. *Nature (Lond.).* 326:77–79.
26. Orci, L., M. Ravazzola, and A. Perrelet. 1984. (Pro)insulin associates with Golgi membranes in pancreatic B cells. *Proc. Natl. Acad. Sci. USA.* 81:6743–6746.
27. Pertoft, H., T. C. Laurent, T. Laas, and K. Lennart. 1978. Density gradients prepared from colloidal silica particles coated by polyvinylpyrrolidone (Percoll). *Anal. Biochem.* 88:271–282.
28. Salpeter, M. M., and M. G. Farquhar. 1981. High resolution analysis of the secretory pathway in mammotrophs of the rat anterior pituitary. *J. Cell Biol.* 91:240–246.
29. Scheele, G., and A. Tartakoff. 1985. Exit of nonglycosylated secretory proteins from the rough endoplasmic reticulum is asynchronous in the exocrine pancreas. *J. Biol. Chem.* 260:926–931.
30. Scheele, G., G. Palade, and A. Tartakoff. 1978. Cell fractionation studies on the guinea pig pancreas. Redistribution of exocrine proteins during tissue homogenization. *J. Cell Biol.* 78:110–130.
31. Sharoni, Y., S. Eimerl, and M. Schramm. 1976. Secretion of old versus new exportable protein in rat parotid slices. Control by neurotransmitters. *J. Cell Biol.* 71:107–122.
32. Tanaka, T., E. W. Gresik, and T. Barka. 1981. Immunocytochemical localization of amylase in the parotid gland of developing and adult rats. *J. Histochem. Cytochem.* 29:1189–1195.
33. Tartakoff, A. M., and P. Vessali. 1978. Comparative studies of intracellular transport of secretory proteins. *J. Cell Biol.* 79:694–707.
34. Tooze, J., and S. A. Tooze. 1986. Clathrin-coated vesicular transport of secretory proteins during the formation of ACTH-containing secretory granules in AtT20 cells. *J. Cell Biol.* 103:839–850.
35. Udenfriend, S., S. Stein, P. Bohlen, W. Dairman, W. Leimgruber, and M. Weigele. 1972. Fluorescamine: a reagent for assay of amino acids, peptides, protein, and primary amines in the picomole range. *Science (Wash. DC).* 178:871–872.
36. Uvnas, B. 1974. The isolation of secretory granules from mast cells. *Methods Enzymol.* 31:395–402.
37. Wagner, J. A., S. S. Carlson, and R. B. Kelly. 1978. Chemical and physical characterization of cholinergic synaptic vesicles. *Biochemistry.* 17:1199–1206.
38. Wallach, D. 1982. The secretory granule of the parotid gland. *In* The Secretory Granule. A. Poisner and J. M. Trifaro, editors. 247–276.
39. Zanini, A., G. Giannatasio, and J. Meldolesi. 1980. Intracellular events in prolactin secretion. *In* Synthesis and Release of Adenohypophyseal Hormones. M. Justuz and K. W. McKerns, editors. 105–123.